6-25-2018

Secondary Electron Yield Measurements of Carbon Nanotube Forests: Dependence on Morphology and Substrate

Brian Wood
Utah State University

Justin Christensen
Utah State University

Gregory Wilson
Utah State University

JR Dennison
Utah State Univesity

T. -C. Shen
Utah State University

SECONDARY ELECTRON YIELD MEASUREMENTS OF CARBON NANOTUBE FORESTS: DEPENDENCE ON MORPHOLOGY AND SUBSTRATE

Brian Wood, Justin Christensen, Greg Wilson, T.C. Shen, and JR Dennison

USU Materials Physics Group, Utah State University
Logan, UT 84321-4415
brian.wood314@gmail.com

Abstract

Total, secondary and backscatter electron yield data were taken with beam energies between 15 eV and 30 keV to determine the extent of suppression of substrate yields caused by carbon nanotube (CNT) forest coatings on substrates. CNT forests are low density graphitic carbon structures of vertically oriented CNT's. Chemical vapor deposition (CVD) was used to grow multi-walled CNT forests between 20-50 μm tall on a thick silicon substrate capped with a 3 nm diffusion barrier of evaporated aluminum. CNT forests can potentially lower substrate yield due both to its low-Z (atomic number) carbon composition, along with its bundled, high aspect ratio architecture. In general, low-Z (atomic number) and low mass density conductors such as carbon have a lower density of bulk electrons for the incident electrons to interact with, thereby reducing the yields. Rough surfaces, and in particular surfaces with deep high-aspect-ratio voids, can also suppress yields as electrons emitted from lower lying surfaces are recaptured by surface protrusions rather than escaping the near-surface region. Modification of yields from coatings can be modeled essentially serially, as layered materials with different yield curves contribute more at certain incident energies. However, it is shown that suppression of the yields due to forest morphology is more significant than simple proportional contributions of components, and is related to the angular distribution of backscattered and secondary electrons as a function of energy. These two effects are expected to be most pronounced at low energies, where the incident electrons interact preferentially with the carbon at the surface.

This study measured yields from three CNT forests of varied height and density, along with yields of an annealed substrate and constituent bulk materials. At incident electron energies above ~1200 eV the substrate yields dominated those of the CNT forests, as incident electrons penetrated through the low-density low-Z CNT forests and backscattered from the higher-Z substrate. At lower energies <1200 eV, the CNT forests substantially reduced the overall yields of the substrate, and for <500 eV CNT forest yields were <1 and well below the already low yields of bulk graphite. The yield's dependence on the height and density of the CNT forest is also discussed. By understanding these effects on electron yield, CNT growth can be catered for specific environments to mitigate spacecraft charging.

I. Introduction

There is significant interest in reducing secondary electron emission from materials used for a variety of applications. This can be done by:

- ***Coating surfaces with intrinsically low-yield materials.*** Low-Z (atomic number) and low mass density conductors such as carbon have a lower density of bulk electrons for the incident electrons to interact with, thereby reducing the yields. Use of colloidal carbon coatings such as Aquadag™ to cover surfaces of electron optics elements and accelerator beam pipes is an example.
- ***Modifying the surface morphology.*** Rough surfaces can also suppress yields, as electrons emitted from lower lying surfaces are recaptured by surface protrusions rather than escaping the near-surface region. The effect of surface roughness on electron yield has even extended to materials of high aspect ratio with deep voids; such an example is carbon velvets which tend to reduce the secondary yield of untreated planar carbon. CNT forest height, density and presence of defects are the main factors expected to have an influence on their ability to absorb stray electrons coming off the substrate and originating within the forest itself.

Carbon nanotube (CNT) forests can potentially lower yield in these ways, exploiting extreme properties of CNT forests. While attempts to measure the secondary yield of individual nanotubes have been made, the present study focuses on the CNT forest samples as a whole, to determine the relative effects on the yield of the material composition and morphology. Forest density, height, and presence of defects are the factors of the morphology that are expected to affect the yield reduction of the sample. Forest density relates to the average packing density of the nanotubes which, along with CNT forest height, determines the density of bulk electrons (C atoms) that the incident electrons to interact and the range that the incident electrons will penetrate into the sample.

II. Forest Growth and Characterization

CNT forests were made in the Utah State University Nanofabrication Lab using a non-plasma enhanced chemical vapor deposition method. Substrates of n-type silicon wafer with a 3 nm layer of evaporated aluminum deposited to produce the proper in-diffusion rate. The wafer was then diced into 1 cm² pieces and loaded into a tube furnace at 700 ºC. A chemical precursor of xylene with a smaller molar concentration of ferrocene was injected into the furnace, dissociating into hydrocarbons and byproducts along with iron atoms from the ferrocene. Hydrogen and argon carrier gas flow into the furnace at 50 sccm facilitated even distribution. Iron atoms coalesced on the substrate to form catalyst particles for free carbons to dissolve into. Duration of growth and precursor volume tend to determine the height of the forest, while the molar concentration of ferrocene in the precursor influences the density of the forest, with higher concentration producing denser forests but more defects.

Scanning Electron Microscopy (SEM) is used to determine the height of the forest, along with its relative density and the presence of defects. Figures 1(a) and 1(b) visually illustrate the differences in density of the denser AlSi 129 sample compared to the AlSi 132 sample. Examples of defects are shown in Figs. 1(c) and 1(d).

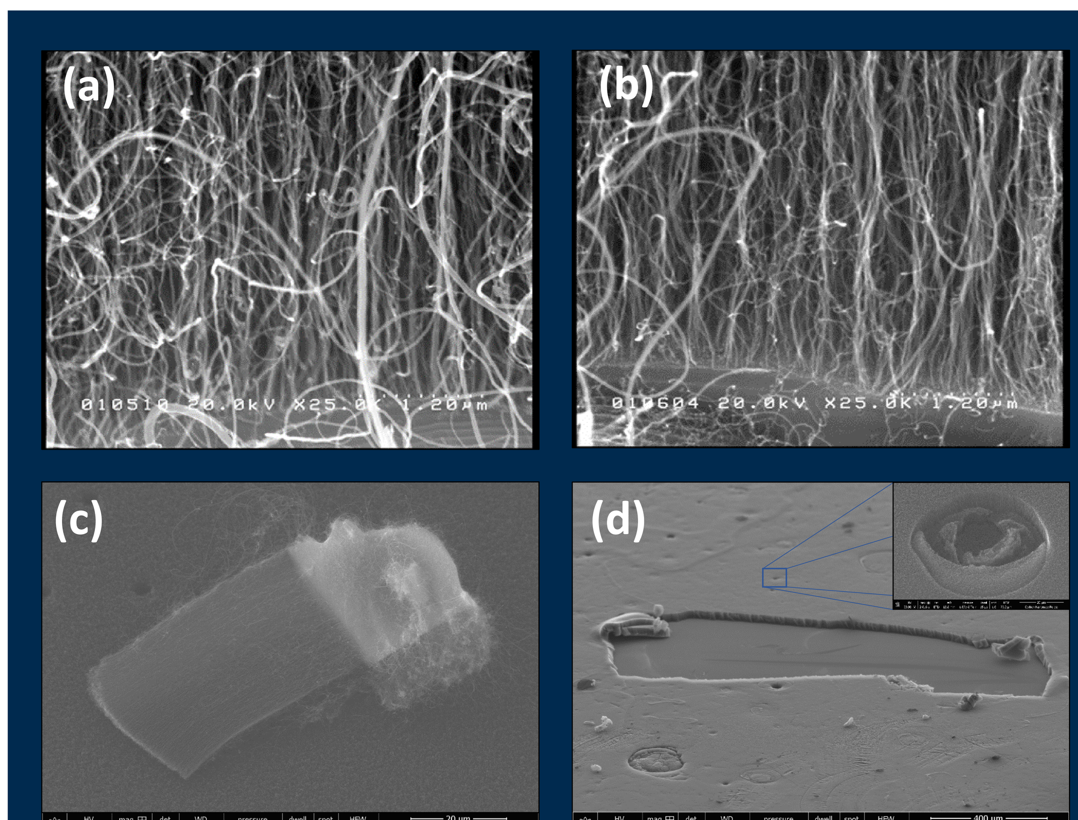

Fig. 1. Bottom side views of AlSi 129 (a) to AlSi 132, comparing the relative density differences due to the difference of ferrocene concentration they were grown with. Typical Examples of defects, a substrate chip (c) that can get dislodged and pushed to the top of the forest, with CNT's still growing off of it, and (d) showing a bad portion with the forest scraped off, with inset of smaller typical surface deformations.

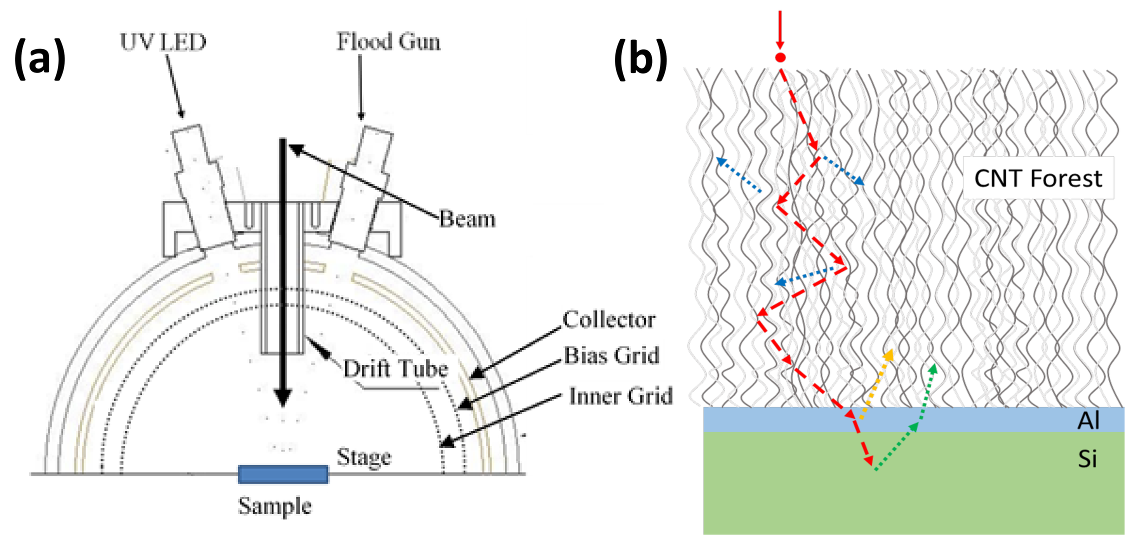

Fig. 2. Schematic of the hemispherical grid retarding field analyzer (a), illustrating the incident beam impinging the sample through the drift tube, along with the inner grid to provide some shielding from a charged sample, the bias grid that can be charged to 50 volts to discriminate backscatter electrons to be captured by the collector. A UV and flood gun may be used to neutralize insulating materials in between data collection that can store charge during electron pulsing. (b) shows possible interactions of incident electrons as it passes through the forest, creating secondary within the forest, aluminum and silicon, which then, depending on the incident energy, get collected by the HGRFA.

Table I: CNT Forest Characteristics

Sample	Height	Ferrocene Concentration (%)	Surface Coverage	Surface Density (μg/cm³)
AlSi 127	24-27	0.5	0.90	~150
AlSi 129	42-51	0.5	0.91	~190
AlSi 132	27-32	0.2	0.82	~160

Values for height, ferrocene concentration and surface coverage are given in Table I. Ferrocene concentration is a relative comparison of density between forests. Surface coverage is also reported by counting the number of pixels above a threshold from top view images of the forest; this is strictly a superficial comparison, as the density varies throughout the forest.

III. Theory and Experimental Setup

Electron yield is an incident energy-dependent measure of the interactions of incident electrons with a material and characterizes the number of electrons emitted per incident electron. The ***total electron yield (TEY)***, is defined as the ratio emitted electron flux to the incident flux,

$$\sigma = \frac{N_{out}^{e-}}{N_{in}^{e-}} = \frac{Q_{out}^{e-}}{Q_{in}^{e-}} \qquad (1)$$

Backscatter electron yield (BSEY) describes electrons emitted from the material which originate from the incident beam; operationally BSE are defined as electrons with emission energies >50 eV.

SE yield (SEY) describes emitted electrons which originate within the material and are excited through inelastic collisions with the incident electrons; operationally SE are defined as electrons with emission energies <50 eV.

Absolute yield were measured using a fully-enclosed hemispherical grid retarding field analyzer (HGRFA) (Fig. 2), which determines absolute yield accurately (<5% absolute uncertainty), since the encapsulating design captures almost all of the emitted electrons. Concentric hemispherical grids are used to energetically discriminate the collected electrons. SEY is calculated as the difference between TEY and BSEY.

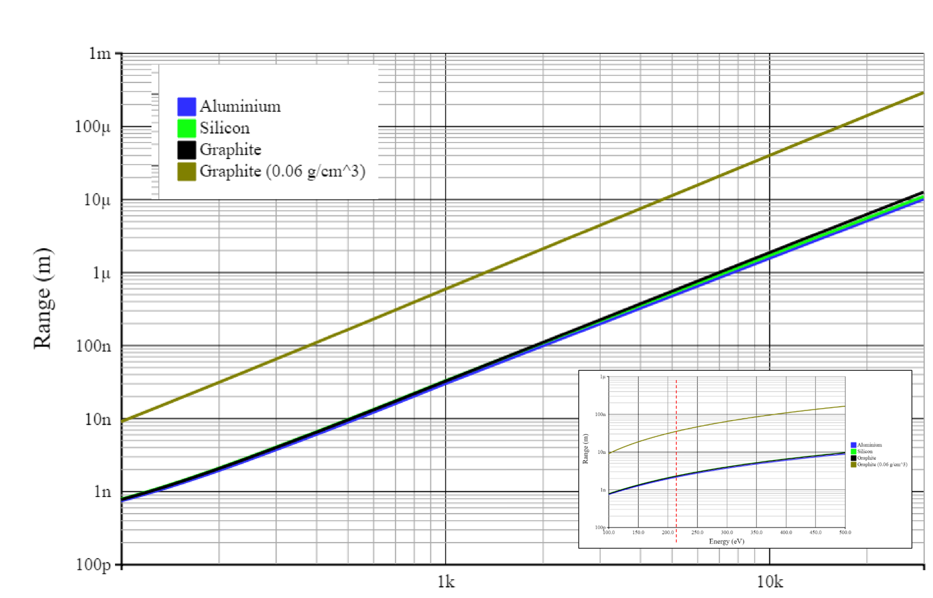

Fig. 3. Log-log graph showing electron range versus incident energy for sample materials Al and Si (indistinguishable on this scale), bulk graphite (density of 2.2 g/cm3), and graphite scaled to 3% of bulk graphite surface density as a surrogate for a material with graphitic composition but density similar to CNT forests. Inset shows the penetration depth of 3 nm for aluminum occurs at 265 eV.

IV. Results and Conclusions

Due to the multi-component nature of the CNT forest-substrate structure, understanding of the yield is done by looking at contributions from all materials individually. The contribution made by bare Si and Al to the AlSi substrate SEY is shown in Fig. 4(a). The penetration depth of Al matches the layer thickness of 3 nm at 265 eV, below which the SEY of Al should dominate. After this energy, Si starts to rule the contribution to the yield, where AlSi SEY lies ~30% above the difference of yields between bare Si and Al, with the rise attributed to secondary electrons still being generated in the thin Al layer.

Fig. 3 shows that the penetration depth of graphite set to ~3% of its normal density does not reach 30 μm until ~8500 eV, a factor of 7 higher than the 1200 eV transition energy seen. This suggests that the effect of the CNTs at low energies is about an order of magnitude large than simple density arguments predict, perhaps due to the CNT morphology. More quantitative measurements of mass density are needed to confirm this. determine how the morphology suppresses substrate yield beyond density arguments.

Total, secondary and backscatter electron yield data of a CNT forest and bulk graphite is seen in Fig. 4(b), taken with beam energies between 15 eV and 30 keV demonstrate that carbon nanotube (CNT) forest coatings on substrates substantially suppress substrate yields. Figure 4(c) at incident electron energies above ~1200 eV shows the substrate yields dominated those of the CNT forests, as incident electrons penetrated through the low-density low-Z CNT forests and backscattered from the higher-Z substrate. Above ~1200 eV, the yield of the forests is slightly higher than the bare substrate, which may result from lower attenuation of SE produced by BSE directed back out of the material. At lower energies <1200 eV, the CNT forests substantially reduced the overall yields of the substrate, and for <500 eV CNT forest yields were <1 and well below the already low yields of bulk graphite. This suggests that the effect of the CNTs at low energies is about an order of magnitude large than simple density arguments predict, perhaps due to the CNT morphology. The yield's dependence on the height and density of the CNT forest is a relatively small effect, but is consistent with increased influence of carbon scatter as the areal density of C atoms increases.

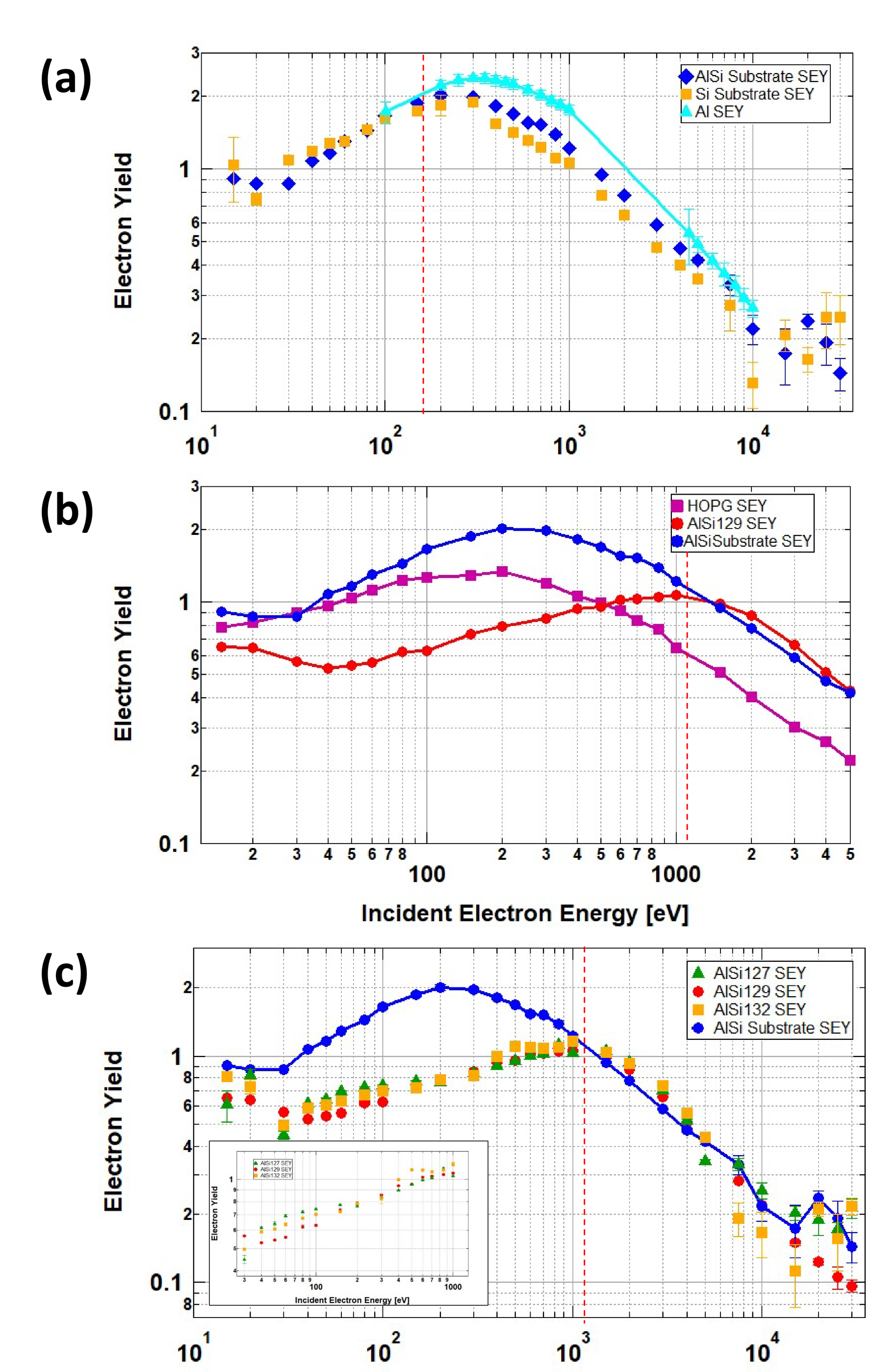

Fig. 4. Secondary electron yield measurements of component sample materials. (a) SEY versus incident energy of bulk Al and uncoated Si substrate, plus a bare coated AlSi substrate. The vertical dashed line indicates the energy of electrons with a 3 nm range. (b) SEY versus incident energy of bulk HOPG graphite, a bare coated AlSi substrate, and an AlSi 129 substrate with CNT forest. (c) Electron yield versus incident electron energy for AlSi 127, AlSi 129 and AlSi 132 CNT forest samples compared to a bare AlSi substrate.

We gratefully acknowledge contributions from other members of the USU Materials Physics Groups.

Scan code to access the USU Material Physics Group papers and presentations.